Segregation of wood particles in a bubbling fluidized bed

Benjamin Cluet, Guillain Mauviel, Yann Rogaume, Olivier Authier, Arnaud Delebarre

Segregation of wood particles in a bubbling fluidized bed

B. Cluet[a], G. Mauviel[b]*, Y. Rogaume[a], O. Authier[c] and A. Delebarre[d]

[a]LERMAB, Université de Lorraine, 27 rue Philippe Séguin; 88051 Epinal, France

[b*] LRGP, CNRS, Université de Lorraine, 1 rue Granville, 54000 Nancy, France

[c] EDF R&D, 6 Quai Watier, 78400 Chatou, France

[d] LEMTA, CNRS, Université de Lorraine, 2 av. de la Forêt de Haye, 54504 Vandoeuvre les Nancy, France

Abstract

Understanding wood segregation in bubbling fluidized beds is of importance for the global analysis, comprehensive modeling, and scale-up of bubbling fluidized bed biomass gasifiers. This study presents measurements of voidage and segregation taken during experiments in fluidized beds containing inert materials mixed with biomass particles. The features of the wood particles affect the bed axial homogeneity; a small particle size or a high density increases homogeneity. When gas velocity is low, the biomass particles are more segregated from olivine compared to the results achieved with larger velocities. In all experiments, a significant portion of the wood remains within the bed (50-80%), while the rest of the biomass floats at the bed surface. The experimental modeling accurately represents the voidage of the bed, with the exception of the upper part of the bed and the floating portion of the biomass particles. The results of the present study are in agreement with recent publications.

Keywords

Fluidization, segregation, biomass, wood, mixing, voidage, pressure analysis

1. Introduction

The gasification or combustion of wood chips in fluidized beds necessitates the use of an inert bed material in which wood particles are introduced. These mixtures of inert materials with "wood/char" particles have complex fluidization behaviors. For instance, Delebarre et al. [1] pointed out that the minimum fluidization velocity concept is not straightforward for these type of binary mixtures.

Understanding wood segregation in bubbling fluidized beds remains important for the global analysis, comprehensive modeling, and scale-up of bubbling fluidized bed gasifiers [2]. This phenomenon is strongly coupled with wood thermochemical reactions (pyrolysis and gasification) and bed hydrodynamics [3]. Segregation is likely to occur when there is a large difference in drag per unit weight between different solid particles.

The segregation of thick wood samples such as chips or pellets in sand beds has been less studied compared to pyrolysis/gasification/combustion kinetics [4–15] or fluidized bed hydrodynamics [1,3,16–21]. Some studies conducted on solid mixing in fluidized beds have focused on particles with the same density but different shapes or diameters [22–24] or particles with the same shape but different densities [22].

Norouzi et al. [25] studied the solid mixing pattern in a bubbling fluidized bed using a radioactive tracer with the same density as the bed material. This radioactive particle tracking method for visualizing the fluidized bed interior is an efficient technique, although it involves complex materials. Recently, Fotovat et al. [26] used the same experimental setup to analyze wood distribution in a sand fluidized bed; measurements were taken with a single tracer particle.

44 They found a wood distribution all along the bed (Figure 9) and better gas mixing with
45 increasing velocity.
46 Wirsum et al. [27] studied light and large particles in sand using a magnetic field to track
47 particles. Vertical mixing was improved by smaller and denser flotsams along with small sand
48 particle diameters and high superficial velocities. Zhang et al. [28] investigated wood
49 segregation and mixing in a fluidized bed. The results were based on three-layer sampling in a
50 bed with a height of 300 mm. They also found that gas velocity affects segregation. In the regime
51 of steady fluidization, mixing and segregation compete with each other, and there is a gas
52 velocity that produces the maximum mixing for any given mixture.
53 Bruni et al. [29] studied the segregation of biomass particles in an incipient bubbling fluidized
54 bed. Biomass particles tend to segregate at the upper part of bed due to endogenous bubbles
55 generated by devolatilization.
56 Some studies have been conducted on lateral mixing in fluidized beds [30–32]. Olsson et al.
57 [31] investigated wood and sand mixing, demonstrating that lateral dispersion is strongly
58 dependent on bubble path. Wood concentration is more significant between bubble paths, and
59 lateral dispersion is higher in the middle part of the bed than close to the surface. In addition,
60 lateral dispersion is lower than vertical dispersion [30].
61 Segregation has often been quantitatively evaluated by a coefficient of segregation or a mixing
62 index. The mixing index is defined by the ratio of the jetsam (i.e., solids that occupy the bottom
63 of the bed) concentration in the upper layer to the average jetsam concentration [33].
64 Experimental evidence [34,35] has shown that the solid composition along the bed is generally
65 not uniquely represented by this ratio. Hemati et al. [34] suggested using a relationship based on
66 the integration of the concentration profile along the bed.

67 The aim of this work is to present an experimental study on axial segregation of thick wood in
68 a relatively large lab-scale bubbling fluidized bed (i.e., diameter of 242 mm) to limit the wall
69 effect (the ratio of the particle equivalent spherical diameter to the bed diameter is at least equal
70 to 18) . As discussed below, some similar experimental studies have already been performed, but
71 previous results were obtained mainly using single particle tracking or thick layer sampling. This
72 study is based on simple pressure analyses and local bed sampling with 50-mm-thick layers. The
73 effects of several parameters related to wood particles are also studied (i.e., size, shape and
74 density). Endogenous bubble formation is not studied herein, even though this phenomenon
75 could impact segregation in real fluidized bed gasifiers.

76 ## 2. Materials, methods and calculation
77 ### 2.1. Materials
78 #### 2.1.1. Experimental device

79 Experiments were carried out in a cold cylindrical fluidized bed composed of five parts: (i) an
80 inlet gas system, (ii) a gas distributor, (iii) a fluidized bed column, (iv) a wood injection system
81 and (v) a data acquisition system. A schematic representation of the experimental setup is given
82 in the Supplementary Material (Figure 1).

83 The fluidized bed was a cylindrical PMMA vessel with an inner diameter of 242 mm, a height
84 of 2.5 m, and a thickness of 8 mm. This vessel was drilled on a vertical line each 50 mm to create
85 pressure transducer inlets. The first hole was drilled 13 mm from the air distributor. Stainless
86 steel pipe (8-mm external diameters, 3-mm internal diameters, and 40-mm lengths) were placed
87 in each of these holes. To prevent bed leakage, filters were inserted in all of the pipes.

88 A PMMA distributor plate with a diameter of 242 mm and a height of 10 mm was perforated
89 by 230 holes with diameters of 2.5 mm arranged in a square pitch in order to uniformly distribute
90 the fluidization gas and avoid channeling and/or slugging. A cloth filter was placed over the air

91 distributor plate to prevent the inert bed particles from falling down. The pressure drop of the air
92 distributor was approximately 2500 Pa at 0.3 m/s.
93 An air box was included between the blower and the distributor plate to homogenize the air
94 flow and obtain good fluidization. This plenum was a cylindrical PMMA vessel with an inner
95 diameter of 242 mm and a height of 510 mm divided by a plate perforated by 5-mm holes. On
96 the upper part of this plate, a layer of stainless steel marbles (15-mm diameter) was employed to
97 homogenize air flow (Supplementary Material Figure 1).
98 The feeding gas was supplied by a side channel blower (MPR, 2.2 kW, 2900 rpm). The blower
99 velocity was controlled by a variable frequency drive (Leroy Somer FMV2304). The velocity of
100 the gas was measured by a hot wire anemometer (0-30 m/s) coupled to a computer for
101 acquisition. The experimental setup was run between 0.04 m/s and 0.55 m/s; this velocity is
102 equivalent to 0.3-6.8 of the minimum fluidization velocity (U_{mf}) depending on the olivine
103 properties.
104 As shown in Figure 1 of the Supplementary Material, the bed was divided into 50-mm-thick
105 layers delimited by pressure pipes. The pressure acquisition system was composed of eight
106 pressure transducers (Honeywell ascx0-5dn and ascx0-1dn) connected to a USB data acquisition
107 device (NI USB-6009). The employed transducers were differential pressure sensors; one input
108 was connected to the bed, while the second input was opened and thus was at ambient pressure.
109 2.1.2. Bed material
110 The inert bed material used in all experiments was composed of non-ferrous olivine (supplied
111 by Sibelco Company North Cape Mineral, Norway). The olivine density and other characteristics
112 are summarized in Table 1. Two types of olivine were used in this study: coarse olivine, which
113 was sieved between 0.25 mm and 0.75 mm before each experiment, and fine olivine, which was

114 passed through 0.25-mm mesh. The fine olivine fraction was fluidized at high velocity (>7 U_{mf})
115 to remove the very fine particles.
116 These particle fractions are the same as those used in hot gasifiers. Using the same particles in a
117 cold fluidized bed implies the failure to comply with the scale-up criteria proposed by Glicksman
118 et al. [36]. However, as mentioned by Leckner et al. [37], it is not a simple task to find perfectly
119 suitable particles to meet these criteria.
120 The olivine particle size distribution (Supplementary Material Figure 3) was measured by laser
121 light scattering with a Malvern Mastersizer Hydro 2000 analyzer. The results obtained from this
122 method were confirmed by comparison with microscope image analysis. These olivine particles
123 were classified as Geldart type B because their size and density ranges were within 40-500 μm
124 and 1400-4500 kg/m^3, respectively. Olivine sphericity was obtained from the image analysis of
125 approximately 400 particles for each type of olivine. For each particle, three diameters were
126 measured: (i) $d_{min,}$ the smallest dimension of particle; (ii) d_{max}, the largest dimension of particle;
127 and (iii) d_{mean}, the mean diameter of particle. Two ratios, $\frac{d_{mean}}{d_{max}}$ and $\frac{d_{min}}{d_{mean}}$, were calculated and
128 are drawn on the Zingg diagram [38] modified by Lees [39] (Supplementary Material Figure 2).
129 2.1.3. Wood
130 Two types of wood were used in the segregation experiments: beech wood (685 kg/m^3), a
131 typical wood for bioenergy applications, and balsa wood (190 kg/m^3), which has approximately
132 the same density as char from beech wood. The advantage of balsa wood is that it is not friable
133 compared to wood char.
134 Two particles shapes were selected for the experiments: cylindrical shape (dowels), with a
135 sphericity equal to 0.77, and chip-like shape, with a sphericity equal to 0.50. These two shapes
136 were chosen to assess the effect of particle shape on segregation. For balsa particles, two sizes

were used to study the effect of size on segregation. All wood properties are summarized in Table 2 and Figure 1.

Three geometrical characteristics (equivalent spherical diameter (d_v), sphericity (Φ_s), and effective diameter (d_{eff})) were calculated from the particle dimensions using Eqs. (1), (2), and (3), respectively.

$$d_v = 2 * \left(\frac{3\pi V_{\text{particle}}}{4}\right)^{\frac{1}{3}} \quad (1)$$

$$\Phi_s = \frac{\pi d_v^2}{S_{particle}} \quad (2)$$

$$d_{eff} = d_v \Phi_s \quad (3)$$

The wood minimum fluidization velocity was calculated using the correlation of Chitester et al. [40] (Appendix 1).

2.2. Experimental method

The experimental setup was run for approximately 30 min with olivine in order to rearrange the bed structure from fixed bed to steady fluidized bed. During this period, the temperature increased slowly inside the bed due to blower air friction, reaching a final temperature of approximately 25°C. The measurements were taken when steady state was achieved.

2.2.1. Minimum fluidization velocity

The minimum fluidization velocity is the smallest superficial gas velocity at which the pressure drop is equal to the bed weight per unit surface area. An olivine bed with a height of 265 mm (20.9 kg) was used to measure the minimum fluidization velocity. After fluidizing the bed vigorously at a high superficial gas velocity (approximately 3.5 U_{mf} for coarse olivine and

155 6.5 U_{mf} for fine olivine), the total pressure drop was measured with "P transducer #1" for
156 different velocity values (from 0.4 m/s to 0 m/s). To determine U_{mf}, a horizontal line
157 corresponding to the average of the high velocity pressure drop was plotted, and a linear fit for
158 low velocity pressure drop was plotted; the intersection of these two lines corresponds to U_{mf}
159 (Supplementary Material Figure 4). This velocity was determined only for the olivine bed. In this
160 study, olivine U_{mf} is used as a reference to characterize inlet gas velocity.

161 2.2.2. Voidage

162 The voidage is the fraction of gas in a bed. This parameter can be defined for the entire bed or
163 for a layer "i" in the bed (Eq. (4)).

$$\epsilon_i = \frac{V_{g,i}}{V_i} \tag{4}$$

164

165 Two technics were used to calculate voidage: one technique for the bed of olivine without wood,
166 and a second for the bed of olivine with wood.

167 Olivine without wood

168 Voidage was calculated from the pressure data (Eq. (5)).

$$\epsilon_{\mathrm{i}} = 1 - \left(\frac{\frac{\Delta P_i}{g.\, h_i}}{\rho_{ol}} \right) \tag{5}$$

169 The voidage calculation requires that two parameters be known: the thickness of each layer and
170 the olivine density. This calculation was performed for all layers except the upper one because its
171 thickness was unknown.

172 Olivine and wood mixture

173 The first experimental method is valid only for a single-component bed. For a binary mixture,
174 the repartition of each type of solid is necessary to determine the voidage. This experiment is
175 divided into two steps. In the first step, the mixture was fluidized for 10 min, and the pressure
176 and velocity were then recorded. The bed expanded slightly during fluidization due to the
177 increase in voidage from the initial voidage to the minimum fluidization voidage. The average
178 bed height during fluidization was $h_{b,f}$. At the end of this step, the air supply was shut down
179 suddenly (0.5 s), and the bed fell down without the rearrangement of particles. The bed height
180 was then equal to the fixed state bed height ($h_{b,s}$).

181 The second experimental step involved the sampling and sieving of each layer in bed. The data
182 were then compared between the fluidization results and the sampling results. It is necessary to
183 calculate an expansion factor f_{exp} (Eq. (6)) that represents the height evolution between the fixed
184 and fluidized states. To compare the results from solid sampling and pressure analysis, it is
185 necessary to extrapolate the sampling data from the height at a fixed state ($h_{b,s}$) to the fluidized
186 height ($h_{b,f}$). This extrapolation induces the assumption that the layer characteristics are
187 identical.

$$f_{exp} = \frac{h_{b,f}}{h_{b,s}} \tag{6}$$

188 This analysis enables the determination of the evolution of the wood fraction in the fluidized bed.
189 All calculations are summarized as follows. The voidage of each layer was calculated by Eq. (7).

$$\epsilon_i = 1 - \frac{\rho_{app,i}}{\rho_{ol}} . \left(1 - \omega_i . \left(1 - \frac{\rho_{ol}}{\rho_w}\right)\right) \tag{7}$$

190 Several parameters are needed for this calculation; the local wood mass fraction ω_i can be
191 deduced using wood mass sampling data for each layer (Eq. (8)).

$$\omega_i = \frac{m_{i,w}}{m_i} \tag{8}$$

192 The wood mass fraction must be calculated for each layer. The height of the layer during sieving
193 is the standstill height and not the fluidized height; to account for this discrepancy, the height of
194 sieving is corrected with f_{exp} (Eq. (9)).

$$h_{i,f} = f_{exp} h_{i,s} \tag{9}$$

195 The apparent density ρ_{app} of each layer was calculated from the determined pressures using Eq.
196 (10).

$$\rho_{app,i} = \frac{\Delta P_i}{g\, h_{i,f}} \tag{10}$$

197 2.2.3. Segregation

198 The segregation experimental methods were the same as those for the voidage calculation of
199 the wood and olivine mixture. The layer wood ratio is defined as the volume of wood in layer
200 "k" to the total volume of wood in bed (Eq. (11)).

$$x_k = \frac{V_{k,w}}{\sum_i V_{i,w}} = \frac{V_{k,w}}{V_w}, \qquad \sum_i x_i = 1 \tag{11}$$

201 Rowe and Nienow [41] used a definition of local mixing index IDM calculated here as the mass
202 ratio of wood particles (ω_i) in the layer divided by the mean mass ratio of wood in the bed ($\overline{\omega}$)
203 (Eq. (12)).

$$IDM_i = \frac{\omega_i}{\overline{\omega}} \tag{12}$$

204 The index IDM was used to calculate the global mixing index M (Eq (13)) [42], where N is the
205 total number of layers in the bed. In this study, the M index was below "1" (perfectly mixed bed)
206 and could have negative values (highly segregated bed).

$$M = 1 - \left(\overline{\omega} \frac{\sum_{i=1}^{N} (IDM_i - 1)^2}{N(1 - \overline{\omega})} \right)^{0.5} \tag{13}$$

This ratio is strongly dependent of the choice of layer thickness. To limit the effect of this choice and obtain an index that varies between 0 and 100%, a new index (H_{moy}) was defined as the average height of wood in the bed divided by the fluidized bed height (Eq.(14)):

$$H_{moy} = \frac{\sum_i V_{w,i} \bar{h}_i}{V_w h_{b,f}} * 100 \quad (14)$$

If wood is totally segregated to the bed surface, H_{moy} tends to 100%, while H_{moy} tends to 0% if the wood is totally segregated near the distributor. If the bed is well mixed, H_{moy} = 50%; however, if H_{moy} = 50%, the bed is not necessarily well mixed. For instance, the segregation of wood particles in the middle of the bed would also lead to H_{moy} = 50%.

3. Results and discussion

The employed operating conditions are summarized in Table 3. For olivine/wood mixtures, the global volume ratio was generally equal to 0.075 $m^3_{wood}/m^3_{wood+olivine}$. According to Fotovat et al. [26], the influence of the global volume ratio on segregation is actually quite low.

3.1. Minimum fluidization velocity

The measured U_{mf} is equal to 0.137 m/s for coarse olivine and 0.082 m/s for fine olivine (Supplementary Material Figure 4). These U_{mf} values correspond to mean diameters (d_v) of 373 µm for coarse olivine and 233 µm for fine olivine calculated by the correlation of Chitester et al. [40] (Appendix 1). These values are very close to the mean diameters measured by Malvern analysis (Table 1).

3.2. Voidage

As explained in section 2.2.2, an expansion factor was calculated from the fixed bed height determination and from the fluidized bed height obtained by pressure measurements. For low velocities (less than 3.15 U_{mf}), the expansion factor f_{exp} was approximately 1.22 regardless of

228 the experimental features. For higher velocities, f_{exp} was approximately 1.25. This variance in
229 f_{exp} is not significant, which make sense because the olivine particles are classified in Geldart
230 group B. Because f_{exp} was quite constant, the global voidage of the bed was also quite constant;
231 however, it is interesting to take a closer look at the local voidage along the bed, which was not
232 uniform.

233 Olivine without wood

234 Figures 2 and 3 show the voidage profiles of the deep and shallow beds of coarse olivine and
235 the shallow bed of fine olivine. For these three series of experiments for olivine without wood,
236 the bottom part (0-60%) of the bed was less porous than the upper part. The highest voidage was
237 found for the layer just below the surface. For fine olivine, the voidage was less variable along
238 the bed height, with a minimum voidage of 0.54 and a maximum voidage of 0.59.

239 Olivine and wood mixture

240 The voidage profiles of olivine and wood mixtures were derived from Eqs. (7)-(10). Figure 2
241 presents the profiles for different mixtures of coarse olivine and wood, indicating that no
242 difference in voidage was observed among all experiments.

243 The voidage trend observed for fine olivine was very different (Figure 3); the voidage
244 decreased with height and was below 60% in the top layer, whereas the voidage exceeded 65%
245 for coarse olivine in the same layer. At 2.15 U_{mf}, the presence of balsa chips affects bed voidage,
246 especially in the upper layer.

247 Figures 2 and 3 also compare the modeling and experimental results. The experimental
248 voidage results differ from the modeling estimates (Appendix 1), which indicate a continuous
249 decrease in voidage with height due to increasing bubble size.

For coarse olivine (Figure 2), the employed correlations are quite good for predicting the voidage at the bottom part of the bed (0-50%); however, in the upper part, the voidage is underestimated. This may be due to bubble splitting near the splash zone, which is not accounted for by the relationships used to estimate voidage. For fine olivine (Figure 3), the prediction is quite good for the bottom part of the bed, where voidage is high; however, the voidage is underestimated all along the bed.

Fotovat et al. [43] demonstrated that the accumulation of biomass particles in the top layers of the bed causes the bubbles to break, whereas the voidage of the emulsion phase significantly deviates from the ϵ_{mf} of olivine due to the abundance of biomass particles in the top half of the bed. Our experiments confirmed these results and showed that the "bubble breakage" phenomenon seems to also occur for olivine alone.

3.3. Segregation

The first set of experiments was carried out using a shallow bed of coarse olivine ($h_{b,s}$ = 265 mm) with four different types of wood and two gas velocities (2.15 U_{mf} and 3.35 U_{mf}). The second set of experiments was performed using a deep bed of coarse olivine ($h_{b,s}$=391 mm) with beech dowels. The third set of experiments was performed with a shallow bed of fine olivine ($h_{b,s}$ = 265 mm) with different velocities and wood shapes. These experiments were performed in order to compare the effects of different features on segregation. To compare the results of the different experiments, H_{moy} was calculated for each experiment (Eq.(14)).

Effect of bed height

The beds were mixtures of coarse olivine and beech dowels with global volume ratios of 0.075 $m^3_{wood}/m^3_{wood+olivine}$ for the shallow bed and 0.099 $m^3_{wood}/m^3_{wood+olivine}$ for the deep bed. Because of this slight difference, it is preferred to compute the layer wood ratio profiles (Figure

4). No major difference in segregation was observed between the two bed heights. H_{moy} differs slightly between the two experiments (64% for the shallow bed and 73% for the deep bed). Wood was present all along the bed, with a higher concentration in the upper part and very few particles close to the gas distributor.

Effect of wood shape

For shape experiments, the bed was composed of coarse olivine (initial bed height = 265 mm, velocity = 2.15 U_{mf}). Figure 5 shows that the mixing was slightly better for the beech chips (H_{moy} = 66%) than for the beech dowels (H_{moy} = 73%). This phenomenon could be explained by the elongated shape of the chips, which allows them to assume vertical positions and sink into the bed.

Effects of wood density

Figure 6 shows the effects of gas velocity and wood density on the segregation for coarse olivine. Two types of wood (balsa, 159 kg/m^3 and beech, 685 kg/m^3) and two velocities (2.15 and 3.35 U_{mf}) were employed. At the low velocity, higher density improved mixing : H_{moy} for beech wood at low velocity was 66%, while that of balsa was 85%. For the higher velocity, density had only a minor effect on segregation phenomena : H_{moy} was 68% for beech wood and 75% for balsa wood. In all cases, the mixing was better for beech particles. The “well mixed line” drawn in Figure 6 represents a constant wood volume fraction (H_{moy} = 50%).

Effect of wood size

Coarse olivine and balsa were used to study the effect of wood size on mixing (Figure 7). Two velocities were used for each particle size. As previously discussed, the higher velocity resulted in better mixing for the large balsa chips : at the low velocity, H_{moy} was 85%, while it was 75% at the high velocity. For small balsa chips, better mixing was also observed at the higher velocity

296 : H_{moy} was 72% at the low velocity, while it was 64% at the high velocity. Size had an effect on
297 segregation : a small wood size improved mixing.

298 Influence of gas velocity

299 The influence of velocity was already shown in Figures 6 and 7. However, in those
300 experiments, the maximum velocity was quite low (3.35 U_{mf}). To further study the effect of
301 velocity on mixing, fine olivine and beech dowels were investigated at three velocities : 2.7, 5,
302 and 6.48 U_{mf} (Figure 8). At the low velocity (2.7 U_{mf}), H_{moy} was 81%, while it was 63% at the
303 medium velocity (5 U_{mf}) and 61% at the high velocity (6.48 U_{mf}). Thus, mixing is increased
304 greatly with increasing velocity.

305

306 All H_{moy} values and their corresponding experimental operating conditions are summarized in
307 Table 3. In all experiments, the partial segregation of wood was observed; a significant mass of
308 wood (20-50%) floated at the bed surface, while the other part (50-80%) was partially mixed in
309 the bed. The reduction in the difference in density between the solids seems to improve mixing at
310 low velocity (i.e., a reduction in biomass particle density increases particle segregation). At a
311 higher velocity, the effect of density seems less important. A smaller wood size also improves
312 mixing. Figure 9 shows that these results are close to those obtained by Fotovat et al. (Table 4)
313 [26] using similar experimental conditions (approximately 3 U_{mf}). The main differences are
314 observed in the upper part of bed; this could be explained by the fact that the wood volume
315 fraction is slightly higher in our study (0.034 m^3_{wood}/m^3_{bed}). The effect of fluidization velocity is
316 less important in our study than in that of Fotovat et al.; however, the velocity range is also
317 different.

318 4. Conclusion

319 This study presents the results of voidage and segregation experiments in fluidized beds of
320 inert materials and wood particles. Two types of inert materials (fine and coarse olivine) with
321 two different minimum fluidization velocities were employed. For the same superficial velocity,
322 the coarse olivine presents a more variable voidage along the height of the bed. These inert
323 materials were then mixed with two types of wood. For the coarse olivine, the presence of wood
324 had no significant effect on the voidage. For fine olivine, the wood affected the voidage,
325 resulting in decreased voidage in the upper part of the bed.
326 The segregation experiments show that the features of the wood affect the axial homogeneity
327 of the mixture: mixing is increased by small particle sphericity and high wood density. The
328 fluidization velocity also affects the mixture: when the velocity was low (<3 U_{mf}), the biomass
329 particles tended to be more segregated than when the velocity was higher than 3 U_{mf} (except for
330 beech chips in coarse olivine). At 6.5 U_{mf}, the mixing quality was only slightly better than at 5
331 U_{mf}. In all experiments, an important portion of the wood remained within the bed (50-80%),
332 while the rest of biomass floated at the bed surface.
333 The voidage of the bottom part of the bed was well represented by usual correlations, while the
334 voidage fraction in the upper part of the bed was underestimated. The results of the present study
335 are in agreement with recently published results in the literature.
336
337 ACKNOWLEDGMENTS
338 The authors acknowledge the financial support of ANR (Agence Nationale de la Recherche) to
339 the GAMECO project that aims to better understand and model biomass gasifiers.
340
341

342 NOMENCLATURE AND UNITS

343 d: diameter (m)

344 IDM : local mixing index

345 f_{exp}: expansion factor (dimensionless)

346 g: gravitational acceleration ($m.s^{-2}$)

347 h: height (m)

348 H_{moy}: average biomass normalized height

349 m: mass (kg)

350 M: global mixing index (dimensionless)

351 ΔP: pressure drop (Pa)

352 u: velocity (m/s)

353 V: volume (m^3)

354 x : wood ratio (m^3_{wood}/ $m^3_{wood\ tot}$)

355

356 Greek symbols

357 ϵ: voidage (dimensionless)

358 n: wood volume fraction ($m^3_{wood}/m^3_{wood+olivine}$)

359 n': wood volume fraction in Fotovat et al. [26] (m^3_{wood}/m^3_{layer})

360 ρ: density ($kg.m^{-3}$)

361 ω: wood fraction (kg_{wood}/ kg_{layer})

362 $\bar{\omega}$: mean wood fraction (kg_{wood}/ kg_{bed})

363 Φ: sphericity (dimensionless)

364

365 Subscripts

366 app: apparent

b: bed

bubble: bubble

eff: effective

f: fluidized

g: gas

i : layer number

max: maximum

mean: mean

min: minimum

mf: minimum fluidization

ol: olivine

p: particle

s: standstill

tot: total (in the whole bed)

v: volume

w: wood

0: initial

385 APPENDICES

386

387 Appendix 1: Hydrodynamics correlations

388 Archimedes number

389 $$Ar = \frac{dp_{ol}^3 \cdot \rho_{gas} g(\rho_{ol} - \rho_{gas})}{{\mu_{gas}}^2}$$

390 Minimum fluidization Reynolds number (Re_{mf}) correlated by Chitester et al. [40]

391 $$Re_{mf} = ((28.7)^2 + 0.0494.Ar)^{0.5} - 28.7$$

392 Minimum fluidization voidage correlated by the Ergun equation [16]

393 $$\frac{1.75}{\epsilon_{mf}^3 . \Phi} . Re_{mf}^2 + \frac{150(1-\epsilon_{mf})}{\epsilon_{mf}^3 . \Phi^2} Re_{mf} = Ar$$

394 Initial bubble diameter correlated by Mori and Wen[44] (cm.s^{-1})

395 $$d_{bubble_0} = \frac{2.78}{10^2 g}\Big((u_{gas} - u_{mf})\Big)^2$$

396 Maximum bubble diameter correlated by Mori and Wen[44] (cm.s^{-1})

397 $$d_{bubble_{max}} = 0.652\left(\frac{\pi}{4} d_{bottom}^2 (u_{gas} - u_{mf})\right)^{0.4}$$

398 Bubble diameter at height "h" correlated by Mori and Wen [44] (cm.s^{-1})

399 $$d_{bubble} = d_{bubble_{max}} - e^{\frac{0.3h}{d_{bed}}}(d_{bubble_{max}} - d_{bubble_0})$$

Single bubble velocity correlated by Davidson and Harrison [45] ($cm.s^{-1}$)

$$u_{br} = 0.711(g.d_{bubble})^{0.5}$$

Bubble velocity correlated by Davidson and Harrison [45] ($cm.s^{-1}$)

$$u_{bubble} = u_{br} + (u_{gas} - u_{mf})$$

Bubble fraction in the bed with deviation factor (Y) from two-phase theory.

$$frac_{bubble} = Y\frac{\left(u_{gas_{bm}} - u_{mf_{ol}}\right)}{u_{bubble}}$$

Deviation factor from two-phase theory [46]

$$Y = 2.27Ar^{-0.21}$$

Emulsion voidage from two-phase theory:

$$\epsilon_{emulsion} = \epsilon_{mf}$$

The average voidage of bed is calculated as follows:

$$\epsilon = frac_{bubble} + (1 - frac_{bubble})\epsilon_{emulsion}$$

Appendix 2: Supplementary materials

AUTHOR INFORMATION

Corresponding Author

*Corresponding author: guillain.mauviel@univ-lorraine.fr.

REFERENCES

[1] A.B. Delebarre, A. Pavinato, J.C. Leroy, Fluidization and mixing of solids distributed in size and density, Powder Technol. 80 (1994) 227–233. doi:10.1016/S0032-5910(94)80007-3.

[2] H. Cui, J.R. Grace, Fluidization of biomass particles: A review of experimental multiphase flow aspects, Chem. Eng. Sci. 62 (2007) 45–55. doi:10.1016/j.ces.2006.08.006.

[3] A. Gomez-Barea, B. Leckner, Modeling of biomass gasification in fluidized bed, Prog. Energy Combust. Sci. 36 (2010) 444–509. doi:10.1016/j.pecs.2009.12.002.

[4] O. Authier, M. Ferrer, G. Mauviel, A.-E. Khalfi, J. Lédé, Wood Fast Pyrolysis: Comparison of Lagrangian and Eulerian Modeling Approaches with Experimental Measurements, Ind Eng Chem Res. 48 (2009) 4796–4809. doi:10.1021/ie801854c.

[5] A. Dufour, P. Girods, E. Masson, Y. Rogaume, A. Zoulalian, Synthesis gas production by biomass pyrolysis: Effect of reactor temperature on product distribution, Int. J. Hydrog. Energy. 34 (2009) 1726–1734. doi:10.1016/j.ijhydene.2008.11.075.

[6] M. Corbetta, A. Frassoldati, H. Bennadji, K. Smith, M.J. Serapiglia, G. Gauthier, et al., Pyrolysis of Centimeter-Scale Woody Biomass Particles: Kinetic Modeling and Experimental Validation, Energy Fuels. 28 (2014) 3884–3898. doi:10.1021/ef500525v.

[7] E. Ranzi, M. Corbetta, F. Manenti, S. Pierucci, Kinetic modeling of the thermal degradation and combustion of biomass, Chem. Eng. Sci. 110 (2014) 2–12. doi:10.1016/j.ces.2013.08.014.

[8] E. Ranzi, A. Cuoci, T. Faravelli, A. Frassoldati, G. Migliavacca, S. Pierucci, et al., Chemical Kinetics of Biomass Pyrolysis, Energy Fuels. 22 (2008) 4292–4300. doi:10.1021/ef800551t.

[9] P. Pepiot, C.J. Dibble, T.D. Foust, Computational Fluid Dynamics Modeling of Biomass Gasification and Pyrolysis, in: American Society, Washington DC, 2010. doi:10.1021/bk-2010-1052.ch012.

[10] R. Radmanesh, Y. Courbariaux, J. Chaouki, C. Guy, A unified lumped approach in kinetic modeling of biomass pyrolysis, Fuel. 85 (2006) 1211–1220. doi:10.1016/j.fuel.2005.11.021.

[11] D. Fiaschi, M. Michelini, A two-phase one-dimensional biomass gasification kinetics model, Biomass Bioenergy. 21 (2001) 121–132. doi:10.1016/S0961-9534(01)00018-6.

[12] M. Puig-Arnavat, J.C. Bruno, A. Coronas, Review and analysis of biomass gasification models, 14 (2010) 2841–2851.

[13] F. Scala, R. Chirone, P. Salatino, Combustion and Attrition of Biomass Chars in a Fluidized Bed, Energy Fuels. 20 (2006) 91–102. doi:10.1021/ef050102g.

[14] O. Senneca, Kinetics of pyrolysis, combustion and gasification of three biomass fuels, Fuel Process. Technol. 88 (2007) 87–97. doi:10.1016/j.fuproc.2006.09.002.

[15] F. Scala, P. Salatino, R. Chirone, Fluidized Bed Combustion of a Biomass Char (Robinia pseudoacacia), Energy Fuels. 14 (2000) 781–790. doi:10.1021/ef9901701.

[16] S. Ergun, Fluid flow through packed columns, Chem Eng Prog. 48 (1952) 89.

[17] C. Y. Wen, Y.H. Yu, A generalized method for predicting the minimum fluidization velocity, AIChE J. 12 (1966) 610–612. doi:10.1002/aic.690120343.

[18] K.S. Lim, J.X. Zhu, J.R. Grace, Hydrodynamics of gas-solid fluidization, Int. J. Multiph. Flow. 21, Supplement (1995) 141–193. doi:10.1016/0301-9322(95)00038-Y.

461 [19] Q. Wang, W. Yin, B. Zhao, H. Yang, J. Lu, L. Wei, The segregation behaviors of fine
462 coal particles in a coal beneficiation fluidized bed, Fuel Process. Technol. 124 (2014) 28–
463 34. doi:10.1016/j.fuproc.2014.02.015.
464 [20] F. Parveen, S. Josset, C. Briens, F. Berruti, Effect of size and density on agglomerate
465 breakage in a fluidized bed, 231 (2012) 102–111. doi:10.1016/j.powtec.2012.07.055.
466 [21] T. Baron, C.L. Briens, P. Galtier, M.A. Bergougnou, Verification of models and
467 correlations for bubble properties in fluidized beds, Chem. Eng. Sci. 45 (1990) 2227–
468 2233. doi:10.1016/0009-2509(90)80099-Z.
469 [22] L.T. Fan, Y. Chang, Mixing of Large Particles in Two Dimensional Gas Fluidized Beds,
470 Can. J. Chem. Eng. 57 (1979) 88–97. doi:10.1002/cjce.5450570114.
471 [23] K. Yoshida, H. Kameyama, F. Shimizu, Mechanism of particle mixing and segregation in
472 gas fluidised beds, in: Fluidization, Springer US, J.R. Grace and J.M. Matsen, New York,
473 1980: pp. 389–396.
474 [24] M.J.V. Goldschmidt, J.M. Link, S. Mellema, J.A.M. Kuipers, Digital image analysis
475 measurements of bed expansion and segregation dynamics in dense gas-fluidised beds,
476 Powder Technol. 138 (2003) 135–159. doi:10.1016/j.powtec.2003.09.003.
477 [25] H.R. Norouzi, N. Mostoufi, Z. Mansourpour, R. Sotudeh-Gharebagh, J. Chaouki,
478 Characterization of solids mixing patterns in bubbling fluidized beds, IChemE. 89 (2011)
479 817–826. doi:10.1016/j.cherd.2010.10.014.
480 [26] F. Fotovat, J. Chaouki, J. Bergthorson, Distribution of large biomass particles in a sand-
481 biomass fluidized bed: Experiments and modeling, AIChE J. 60 (2014) 869–880.
482 doi:10.1002/aic.14337.
483 [27] M. Wirsum, F. Fett, N. Iwanowa, G. Lukjanow, Particle mixing in bubbling fluidized
484 beds of binary particle systems, Powder Technol. 120 (2001) 63–69. doi:10.1016/S0032-
485 5910(01)00348-5.
486 [28] Y. Zhang, B. Jin, W. Zhong, Experimental investigation on mixing and segregation
487 behavior of biomass particle in fluidized bed, Chem. Eng. Process. 48 (2009) 745–754.
488 doi:10.1016/j.cep.2008.09.004.
489 [29] G. Bruni, R. Solimene, A. Marzocchella, P. Salatino, J. Yates, P. Lettieri, et al., Self-
490 segregation of high-volatile fuel particles during devolatilization in a fluidized bed reactor,
491 128 (2002) 11–21.
492 [30] L. Shen, J. Xiao, F. Niklasson, F. Johnsson, Biomass mixing in a fluidized bed biomass
493 gasifier for hydrogen production, Chem. Eng. Sci. 62 (2007) 636–643.
494 doi:10.1016/j.ces.2006.09.033.
495 [31] J. Olsson, D. Pallarès, F. Johnsson, Lateral fuel dispersion in a large-scale bubbling
496 fluidized bed, Chem. Eng. Sci. 74 (2012) 148–159. doi:10.1016/j.ces.2012.02.027.
497 [32] J.C. Abanades, G.S. Grasa, Modeling the Axial and Lateral Mixing of Solids in Fluidized
498 Beds, Ind. Eng. Chem. Res. 40 (2001) 5656–5665. doi:10.1021/ie0009278.
499 [33] A.W Nienow, T Chiba, Fluidization of Dissimilar Materials, in: Fluid. 2nd Ed, Academic
500 Press, J.F Davidson, R.Clift and Harrison, London, 1985.
501 [34] M. Hemati, K. Spieker, C. Laguérie, R. Alvarez, F.A. Riera, Experimental study of
502 sawdust and coal particle mixing in sand or catalyst fluidized beds, Can. J. Chem. Eng. 68
503 (1990) 768–772. doi:10.1002/cjce.5450680505.
504 [35] A. Marzocchella, P. Salatino, V.D. Pastena, L. Lirer, Fluidization in Pyroclastic Flow, in:
505 Ninth Eng. Found. Conf. Fluid., Engineering Foundation, Durango, Colorado, 1998: p.
506 389/788.

[36] L.R. Glicksman, M.R. Hyre, P.A. Farrell, Dynamic similarity in fluidization, Int. J. Multiph. Flow. 20, Supplement 1 (1994) 331–386. doi:10.1016/0301-9322(94)90077-9.
[37] B. Leckner, P. Szentannai, F. Winter, Scale-up of fluidized-bed combustion : A review, 90 (2011) 2951–2964. doi:10.1016/j.fuel.2011.04.038.
[38] Zingg, Beitrag zur Schotteranalys, Universitaet Zuerich, 1935.
[39] G. Lees, The measurement of particle shape and its influence in engineering materials., J. Br. Granite Whinestone Fed. (1964) 1–22.
[40] D.C. Chitester, R.M. Kornosky, L.-S. Fan, J.P. Danko, Characteristics of fluidization at high pressure, Chem. Eng. Sci. 39 (1984) 253–261. doi:10.1016/0009-2509(84)80025-1.
[41] P.N. Rowe, A.W. Nienow, The mechanism by which particles segregate in gas fluidised beds-binary systems of near-spherical particles, Trans Inst Chem Eng. 50 (1972) 310–323.
[42] A. Michaels, V. Puzinauskas, Evaluation performance characteristics of mecanical mixing processes the dextrose kaolinite water system, Chem. Eng. Prog. 50 (1954) 604–614.
[43] F. Fotovat, J. Chaouki, J. Bergthorson, The effect of biomass particles on the gas distribution and dilute phase characteristics of sand–biomass mixtures fluidized in the bubbling regime, Chem. Eng. Sci. 102 (2013) 129–138. doi:10.1016/j.ces.2013.07.042.
[44] S. Mori, C.Y. Wen, Estimation of bubble diameter in gaseous fluidized beds, AIChE J. 21 (1975) 109–115. doi:10.1002/aic.690210114.
[45] J.F. Davidson, D. Harrison, Fluidized Particles, Cambridge Univ. Press, New York, 1963.
[46] S.Y. Wu, J. Baeyens, Segregation by size difference in gas fluidized beds, Powder Technol. 98 (1998) 139–150. doi:10.1016/S0032-5910(98)00026-6.

541 FIGURE CAPTIONS

542 Figure 1. Pictures of wood particles
543 Figure 2. Bed voidage axial profiles with coarse olivine ($h_{b,s}$=265 mm or 391 mm, gas velocity =
544 2.15 U_{mf}, with or without beech dowels)
545 Figure 3. Bed voidage axial profiles with fine olivine ($h_{b,s}$=265 mm, gas velocity = 2.7-6.48 U_{mf},
546 with or without small chips balsa or beech dowels)
547 Figure 4. The effect of bed height on the segregation profiles ($h_{b,s}$=265 mm or 391 mm, coarse
548 olivine, gas velocity = 2.15 U_{mf}, with beech dowels)
549 Figure 5. The effect of wood shape on segregation profiles ($h_{b,s}$=265 mm, coarse olivine, gas
550 velocity = 2.15 U_{mf}, with beech chips or dowels)
551 Figure 6. The effects of wood density on segregation profiles ($h_{b,s}$=265 mm, coarse olivine, gas
552 velocity = 2.15 or 3.35 U_{mf}, beech or balsa chips)
553 Figure 7. The effect of wood size on segregation profiles ($h_{b,s}$=265 mm, coarse olivine, gas
554 velocity = 2.15 or 3.35 U_{mf}, small or large balsa chips)
555 Figure 8. The effect of gas velocity on segregation profiles ($h_{b,s}$=265 mm, fine olivine, gas
556 velocity = 2.7-6.48 U_{mf}, with beech dowels)
557 Figure 9. Comparison of the segregation profiles from this study with those of Fotovat et al. [28]
558

559 APPENDIX 2

560 Figure 1. Simplified scheme of the experimental setup
561 Figure 2. Olivine sphericity estimated from Zingg [37] and modified by Lees [38] diagram (×:
562 fine olivine, +: coarse olivine)
563 Figure 3. Olivine size distribution measured by Malvern analysis
564 Figure 4. Minimum fluidization velocity
565

566 TABLE CAPTION

567 Table 1. Olivine features
568 Table 2. Wood properties
569 Table 3. Summary of experimental conditions and H_{moy} values
570 Table 4. Experimental conditions of Fotovat et al. [26]
571

572

Table 1

Material	Particle density (kg/m^3)	Diameter (μm)	Sphericity	U_{mf} (m/s)
Coarse Olivine	3250	378	0.82	0.137
Fine Olivine	3250	237	0.78	0.082

Table 2

Material	Density (kg/m^3)	Dimension (mm) ±0.1 mm	Sphericity	d_v (m)	d_{eff} (m)	Calculated U_{mf} at 25°C (m/s)
Beech	685	8 (diam.) * 25 Dowels	0.77	$1.34.10^{-2}$	$1.03.10^{-2}$	1.54
Beech	685	5.5 * 4 * 57 Large chips	0.50	$1.34.10^{-2}$	$0.76.10^{-2}$	1.30
Balsa	159	5.5 * 4 * 57 Large chips	0.50	$1.34.10^{-2}$	$0.76.10^{-2}$	0.59
Balsa	159	2 * 4 * 29.5 Small chips	0.50	$0.76.10^{-2}$	$0.38.10^{-2}$	0.34

Table 3

Figure #	U/U_{mf}	Olivine	Initial bed height $h_{b,s}$ (mm)	Wood species	Shape	Wood volume / (olivine + wood volume) (%)	H_{moy}
8	6.48	fine	265	beech	dowels	7.5	61 %
8	5.04	fine	265	beech	dowels	7.5	63 %
4	2.15	coarse	391	beech	dowels	9.9	64 %
7	3.35	coarse	265	balsa	small chips	8.7	64%
5, 6	2.15	coarse	265	beech	chips	7.5	66 %
6	3.35	coarse	265	beech	chips	7.5	68 %
7	2.15	coarse	265	balsa	small chips	8.7	72 %
4, 5	2.15	coarse	265	beech	dowels	7.5	73 %
6, 7	3.35	coarse	265	balsa	chips	8.7	75 %
8	2.70	fine	265	beech	dowels	7.5	81 %
6, 7	2.15	coarse	265	balsa	chips	8.7	85 %

Table 4

Wood volume ratio (m^3_{wood}/m^3_{bed})	Wood density (kg/m^3)	Wood dimension (mm)	Sand density (kg/m^3)	Sand mean diameter (μm)
0.0356 and 0.1359	824	6.35 (diam) * 12.70	2650	380

Figure 1

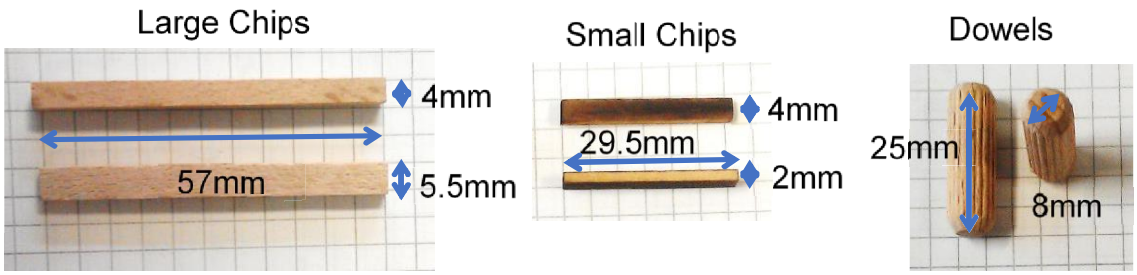
Large Chips
4mm
57mm
5.5mm
Small Chips
4mm
29.5mm
2mm
Dowels
25mm
8mm

Figure 2

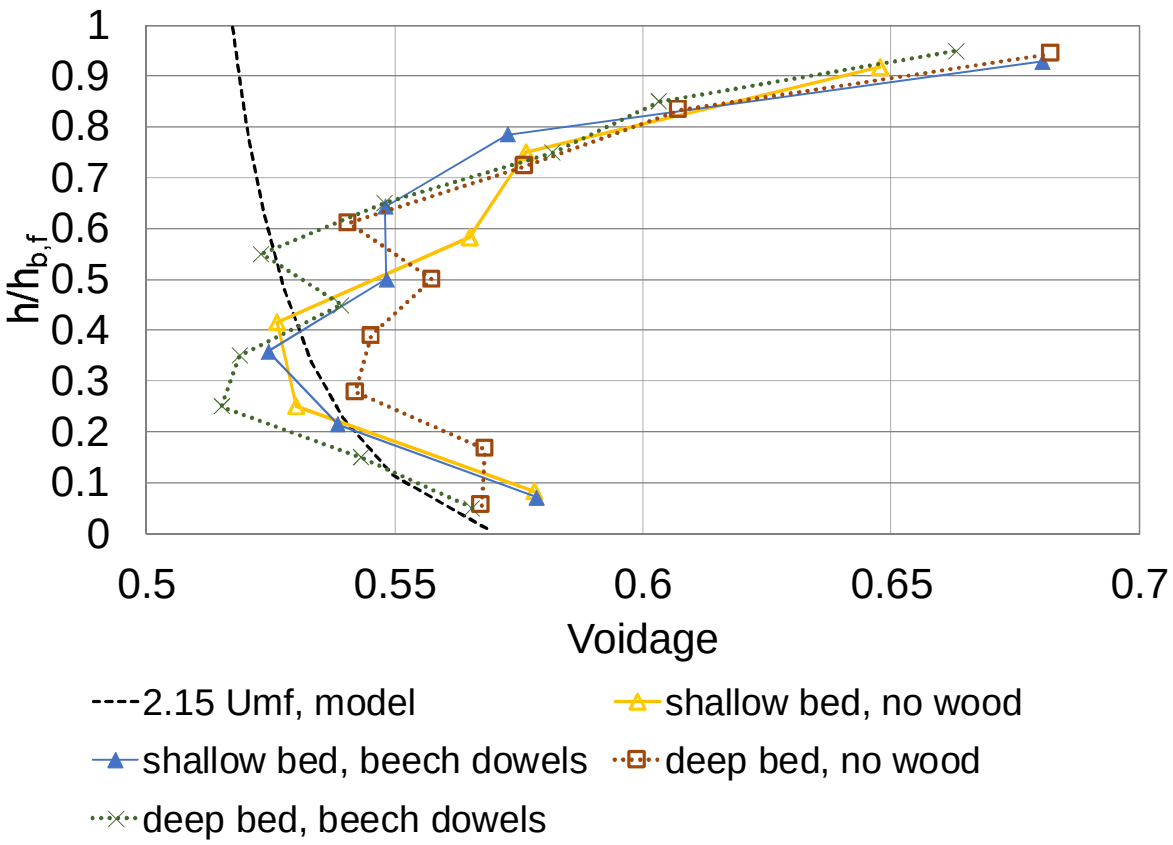
1
0.9
0.8
0.7
0.6
0.5
0.4
0.3
0.2
0.1
0
h/h_b,f
0.5
0.55
0.6
0.65
0.7
Voidage
2.15 Umf, model
shallow bed, no wood
shallow bed, beech dowels
deep bed, no wood
deep bed, beech dowels

Figure 3

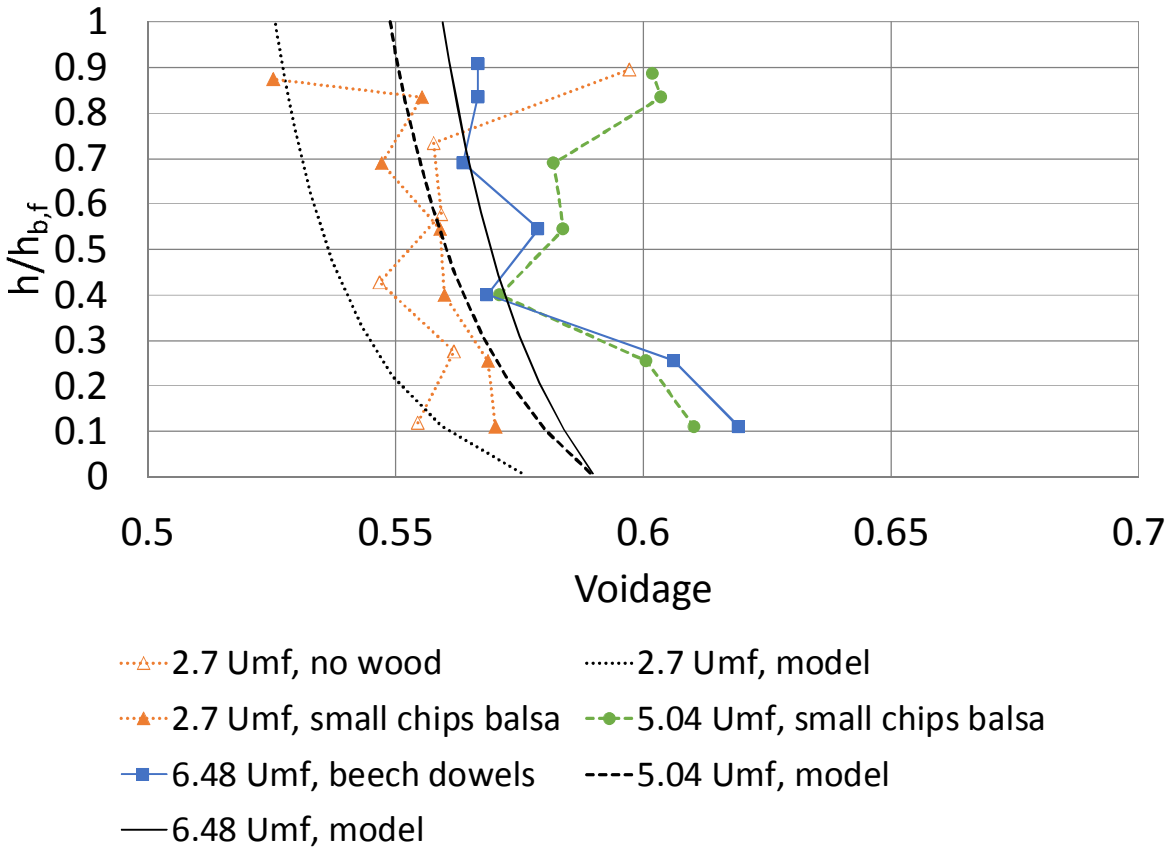
1
0.9
0.8
0.7
0.6
0.5
0.4
0.3
0.2
0.1
0
h/h_b,f
0.5
0.55
0.6
0.65
0.7
Voidage
2.7 Umf, no wood
2.7 Umf, model
2.7 Umf, small chips balsa
5.04 Umf, small chips balsa
6.48 Umf, beech dowels
5.04 Umf, model
6.48 Umf, model

Figure 4

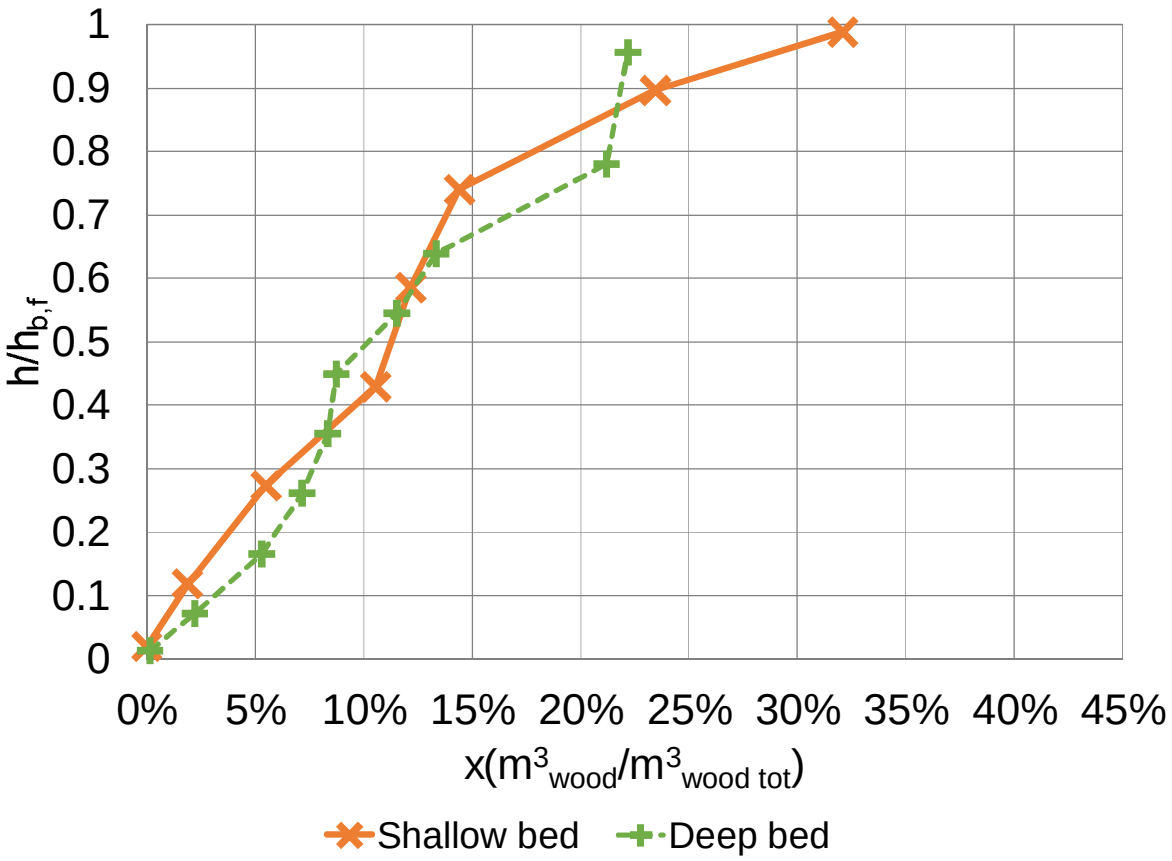
1
0.9
0.8
0.7
0.6
0.5
0.4
0.3
0.2
0.1
0
h/h_b,f
0%
5%
10%
15%
20%
25%
30%
35%
40%
45%
x(m3wood/m3wood tot)
Shallow bed
Deep bed

Figure 5

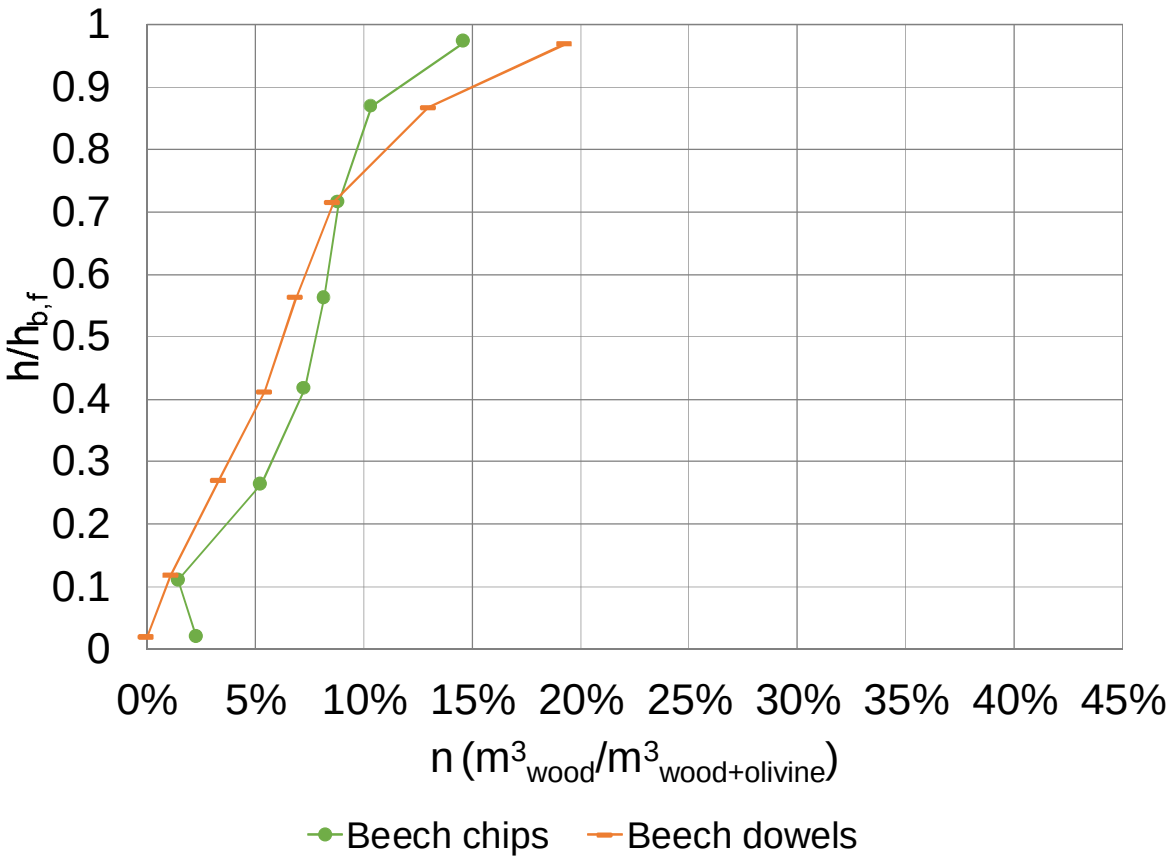
1
0.9
0.8
0.7
0.6
0.5
0.4
0.3
0.2
0.1
0
h/h_b,f
0%
5%
10%
15%
20%
25%
30%
35%
40%
45%
n (m3wood/m3wood+olivine)
Beech chips
Beech dowels

Figure 6

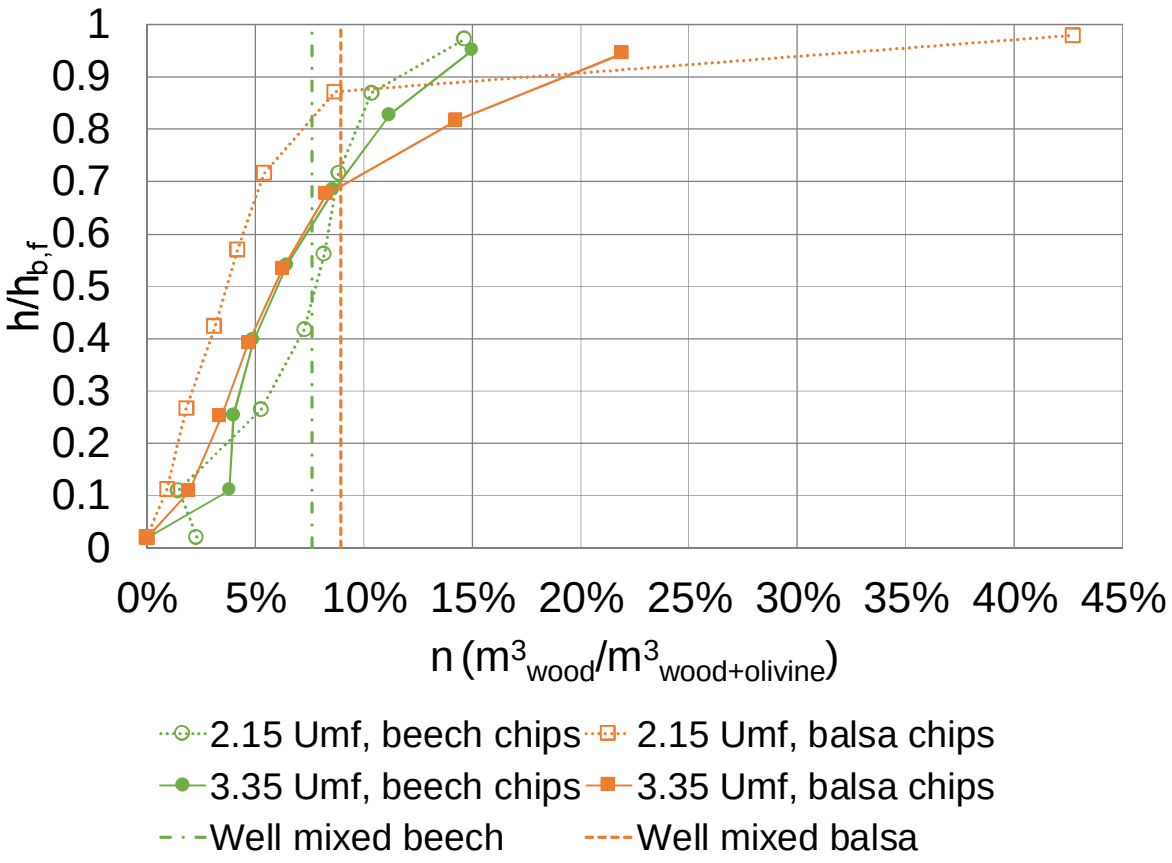
1
0.9
0.8
0.7
0.6
0.5
0.4
0.3
0.2
0.1
0
h/h_b,f
0%
5%
10%
15%
20%
25%
30%
35%
40%
45%
n (m3wood/m3wood+olivine)
2.15 Umf, beech chips
2.15 Umf, balsa chips
3.35 Umf, beech chips
3.35 Umf, balsa chips
Well mixed beech
Well mixed balsa

Figure 7

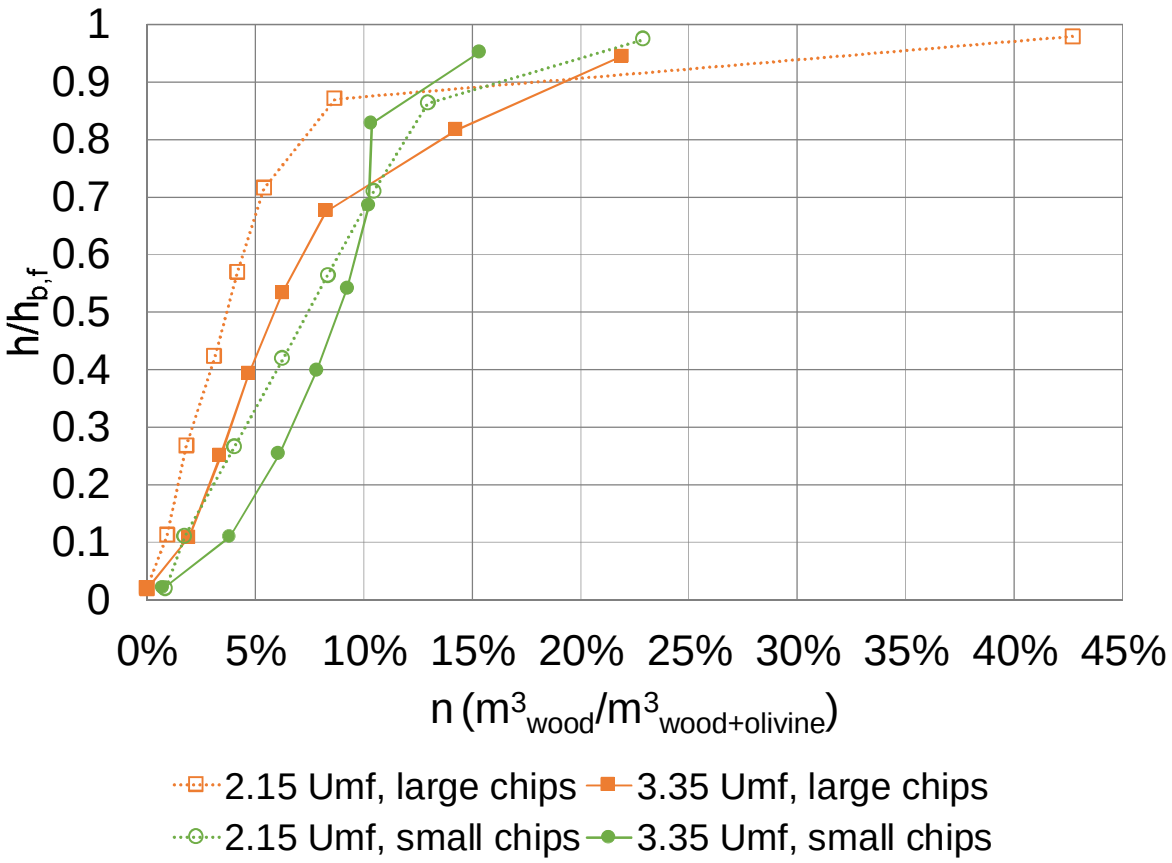
1
0.9
0.8
0.7
0.6
0.5
0.4
0.3
0.2
0.1
0
h/h_b,f
0%
5%
10%
15%
20%
25%
30%
35%
40%
45%
n (m3wood/m3wood+olivine)
2.15 Umf, large chips
3.35 Umf, large chips
2.15 Umf, small chips
3.35 Umf, small chips

Figure 8

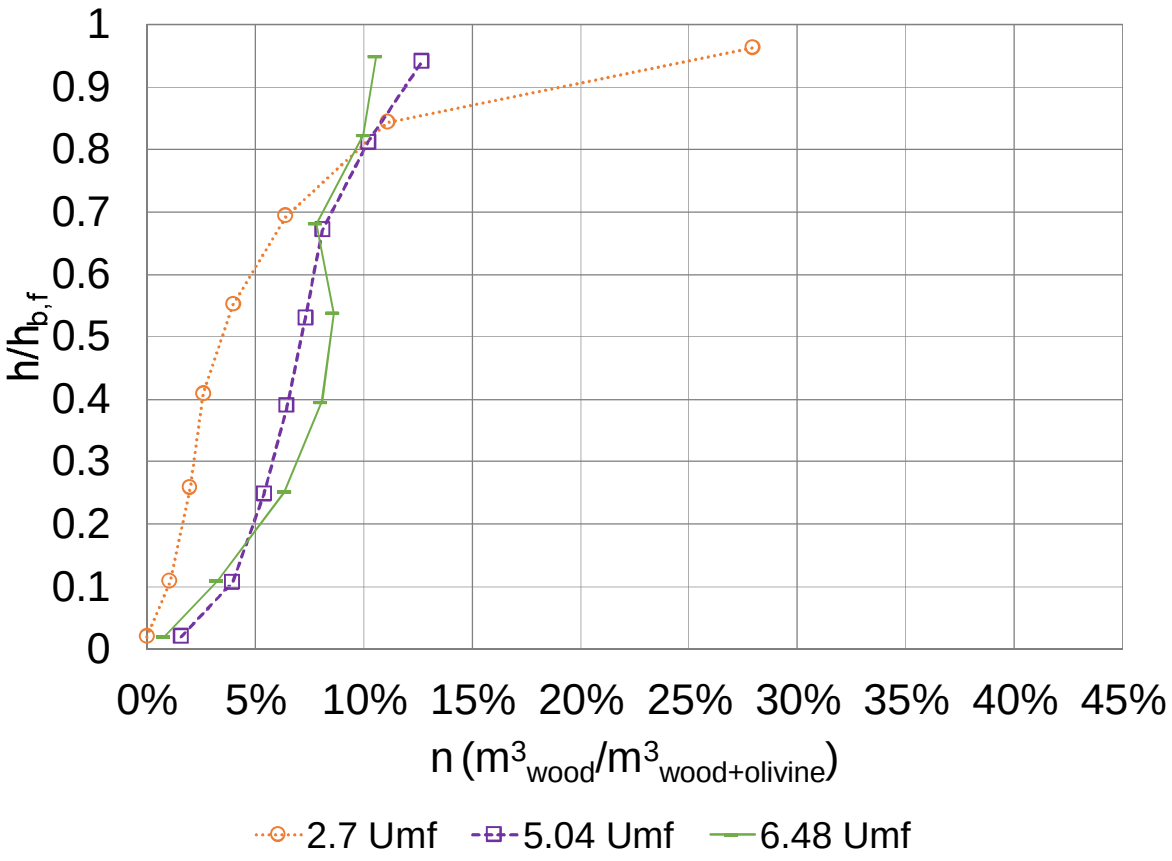
1
0.9
0.8
0.7
0.6
0.5
0.4
0.3
0.2
0.1
0
h/h_b,f
0%
5%
10%
15%
20%
25%
30%
35%
40%
45%
n (m3wood/m3wood+olivine)
2.7 Umf
5.04 Umf
6.48 Umf

Figure 9

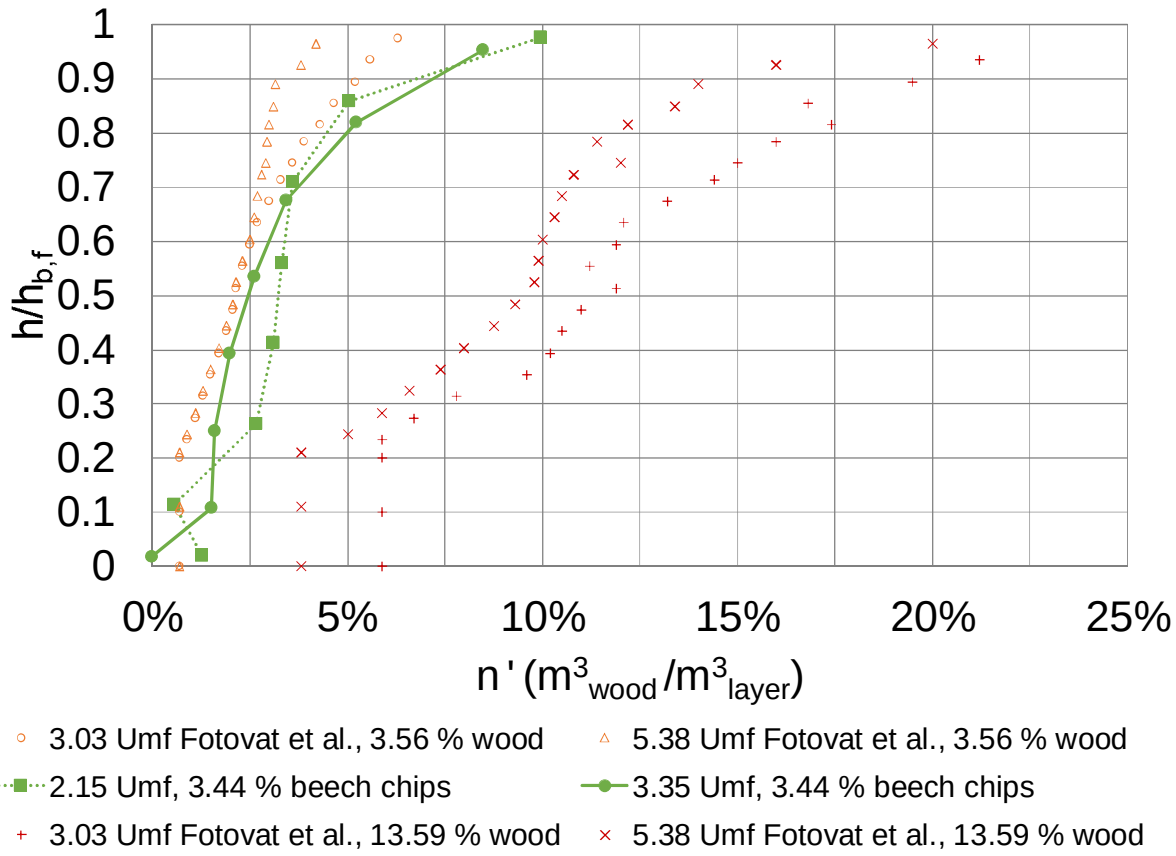
1
0.9
0.8
0.7
0.6
0.5
0.4
0.3
0.2
0.1
0
h/h_b,f
0%
5%
10%
15%
20%
25%
n ' (m3wood /m3layer)
3.03 Umf Fotovat et al., 3.56 % wood
5.38 Umf Fotovat et al., 3.56 % wood
2.15 Umf, 3.44 % beech chips
3.35 Umf, 3.44 % beech chips
3.03 Umf Fotovat et al., 13.59 % wood
5.38 Umf Fotovat et al., 13.59 % wood